9th ANKARA INTERNATIONAL AEROSPACE CONFERENCE **AIAC-2017-159**

20-22 September 2017 - METU, Ankara TURKEY

DYNAMICAL MODELING OF A HORIZONTAL AXIS WIND TURBINE SYSTEM WITH PRECONE AND TILT ANGLES

Mustafa Sahin[1] Ilkay Yavrucuk[2]

Middle East Technical University
Ankara, Turkey

ABSTRACT

This paper explains the development of a dynamical nonlinear horizontal axis wind turbine (HAWT) modeling based on BEM theory with precone and tilt angles. All the implementations are carried out in Matlab and Simulink software for the NREL 5MW wind turbine configuration. Comparison of the model is realized using previously published data.

Nomenclature

a	Axial Induction Factor
a'	Angular Induction Factor
a_c	Critical Axial Induction Factor
B	Blade Number
R	Rotor Radius
r	Local Rotor Radius
c	Local Chord Length
ρ	Air Density
U	Freestream Velocity
U_{rel}	Relative Wind Velocity
Ω	Rotor Angular Velocity
Cl	Lift Coefficient
Cd	Drag Coefficient
C_N	Normal Force Coefficient
C_T	Tangential Force Coefficient
dF_N	Elemental Normal (Thrust) Force
dF_T	Elemental Tangential Force
dF'_N, dT	Elemental Total Thrust Force
dF'_T	Elemental Total Tangential Force
dQ	Elemental Total Torque
dF_L	Elemental Lift Force
dF_D	Elemental Drag Force
F_{hub}	Hub Loss Factor
F_{tip}	Tip Loss Factor
F	Total Loss Factor
σ	Local Solidity
φ	Inflow Angle
α	Angle of Attack
X	Wake Skew Angle
Λ	Azimuth Angle
Ψ	Yaw Angle
θ	Tilt Angle
Φ	Precone Angle
θ_T	Elemental Twist Angle
θ_{po}	Blade Pitch Angle
J_t	Total Turbine Inertia
J_{rotor}	Rotor Inertia
J_{gen}	Generator Inertia
N_{gear}	Gearbox Ratio
τ_{aero}	Aerodynamic Rotor Torque
τ_{gen}	Generator Torque with Gearbox Ratio Effect

[1] Research Assistant, Department of Aerospace Engineering, e-mail: musahin@metu.edu.tr

[2] Associate Professor, Department of Aerospace Engineering, e-mail: yavrucuk@metu.edu.tr

INTRODUCTION

Wind turbines are one of the leading systems for the production of electricity in the world as they utilize the low cost clean wind energy. Therefore, the number of installed wind turbines is increasing annually and have reached about 500.000 MW of installed power around the world[GWEC, 2016].

Although wind turbines are designed in different sizes and appearances, (Figure 1) the most commonly used wind turbine is the Horizontal Axis Wind Turbine (HAWT) due to its efficiency [Pao & Johnson, 2009]. A characteristic HAWT consists of a rotor (hub and blades), a drive train (shafts, gear box, couplings, mechanical brake, and electrical generator), a nacelle and the main frame (housing, bedplate and yaw system), electrical and control systems as well as a foundation and a tower that holds the whole system up in the air flow[Singh & Santoso, 2011]. Of all the components, the rotor may be said to be the most vital part of the turbine as it decides the amount of energy captured from the wind. Therefore, the more efficient the blades, the higher the energy obtained by the turbine.

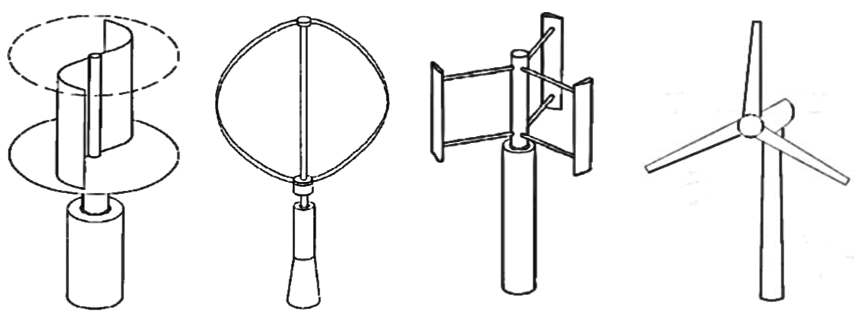

a) Savonius Type　b) Darrieus Type　c) H Type　d) Horizontal Axis Type

Figure 1: Various Types of Turbines [Erich, 2006]

Wind turbine dynamic simulation models that can run in real-time are finding increasing use in the wind power industry. They are employed for predicting turbine performance, developing controller algorithms, testing turbine behavior as a function of time etc.

A popular method to develop such dynamic models is through the use of Blade Element Momentum (BEM) theory. BEM theory is used to predict the wind turbine performance, which is measured in terms of generated power with respect to the freestream velocity or Tip Speed Ratio (TSR). BEM theory is largely utilized due to its ease of implementation and computational effectiveness. Wind properties, turbine and rotor geometric features and blade airfoil data are introduced to the BEM based turbine model as inputs. Therefore, rotor torque, thrust, power and so on are taken as outputs from the model. Often, BEM theory includes some corrections such as tip and hub loss corrections, high axial induction operation correction, skewed wake correction etc. to represent the actual turbine operation.

The purpose of this article is to develop a dynamic nonlinear model for HAWTs based on BEM theory with precone and tilt angles. In addition, the developed HAWT model includes the features of collective and individual blade pitching capabilities along with the nacelle yawing capability. All the implementations have been realized in the Matlab and Simulink software. The NREL 5 MW turbine is used as an example in an attempt to verify the model. The turbine is representative of a utility scale multi-megawatt turbine. It is a three-bladed, upwind, variable-speed as well as a variable blade-pitch-to-feather controlled turbine with precone and tilt angles. Some properties of the NREL 5MW turbine are found in [Jonkman, Butterfield, Musial, & Scott, 2009].

This paper is organized as follows: The next section is about the methodology, which respectively details the BEM theory with corrections, defines the addition of precone and tilt angles along with yawing capability to the model, clarifies the applications of iteration process and all the corrections, and lastly focuses on the dynamical wind turbine model construction. The final section is about the aerodynamic model validation and the discussions.

METHODOLOGY

BEM theory with corrections is employed in order to perform the dynamical modeling of a HAWT model. Various coordinate systems and transformations [Ning, 2013] are realized to construct the wind turbine system. Previous works by [Burton, Sharpe, Jenkins, & Bossanyi, 2001; Manwell, McGowan, & Rogers, 2002; Moriarty & Hansen, 2005; Hansen, 2008; Ceyhan, 2008; Ning, 2013; Ning, Hayman, Damiani, & Jonkman, 2015] are utilized. Comparison of the model is realized with the results given in [Galvani, Sun, & Turkoglu, 2016]. This section details the methodology used for modeling.

Wind Turbine Aerodynamic Modelling-BEM Theory

BEM theory is the combined results of the blade element and momentum theories. In blade element theory, the blade is divided into elements. The aerodynamic forces at every element are determined as a function of blade geometry. Then, these forces are utilized to determine the thrust and torque of the turbine rotor. Momentum theory uses an annular control volume approach for defining the turbine rotor thrust and torque considering the linear and angular momentum conservation principles. Finally, BEM theory uses equations (1 and 2) from momentum theory and equations (3 and 4) from blade element theory to calculate the elemental total thrust and torque of the turbine rotor. Detailed derivations of both theories are given in reference of [Burton et al., 2001; Manwell et al., 2002; Hansen, 2008; Ceyhan, 2008]. Therefore, including the losses due to the effect of three-dimensionality, the thrust and torque equations are derived respectively from the axial and angular momentum conservation principles for each blade element as follows:

$$dT = \rho U^2 4a(1-a)\pi r F dr \tag{1}$$

$$dQ = \rho U 4a'(1-a)\Omega \pi r^3 F dr \tag{2}$$

Similarly, the elemental total thrust and torque from the blade element theory are obtained as,

$$dT = dF'_N = BdF_N = \frac{1}{2} B\rho U_{rel}^2 C_n c dr \tag{3}$$

$$dQ = rdF'_T = rBdF_T = \frac{1}{2} B\rho U_{rel}^2 C_t c r dr \tag{4}$$

Where dF_N and dF_T (Figure 2) are the elemental normal and tangential forces to the plane of blade rotation (Figure 2) and are found as follows.

$$dF_N = \frac{1}{2}\rho U_{rel}^2 C_n c dr \tag{5}$$

$$dF_T = \frac{1}{2}\rho U_{rel}^2 C_t c dr \tag{6}$$

These elemental forces, dF_N and dF_T are found by a transformation of elemental aerodynamic lift, dF_L and drag, dF_D forces (Figure 2). Due to this transformation, the normal and tangential force coefficients, C_n and C_t are taken the following forms.

$$C_n = (C_l \cos\varphi + C_d \sin\varphi) \tag{7}$$

$$C_t = (C_l \sin\varphi - C_d \cos\varphi) \tag{8}$$

And the elemental lift, dF_L and drag, dF_L forces are given by the following equations.

$$dF_L = \frac{1}{2}\rho U_{rel}^2 C_l c dr \tag{9}$$

$$dF_D = \frac{1}{2}\rho U_{rel}^2 C_d c dr \tag{10}$$

By utilizing the geometry depicted in Figure 2, the relative wind, U_{rel}, inflow angle, φ, and angle of attack, α, are computed respectively as follows.

$$U_{rel} = \sqrt{\left(U(1-a)\right)^2 + \left(\Omega r(1+a')\right)^2} \tag{11}$$

$$\varphi = \tan^{-1}\frac{U(1-a)}{\Omega r(1+a')} \tag{12}$$

$$\alpha = \varphi - (\theta_T + \theta_{po}) \tag{13}$$

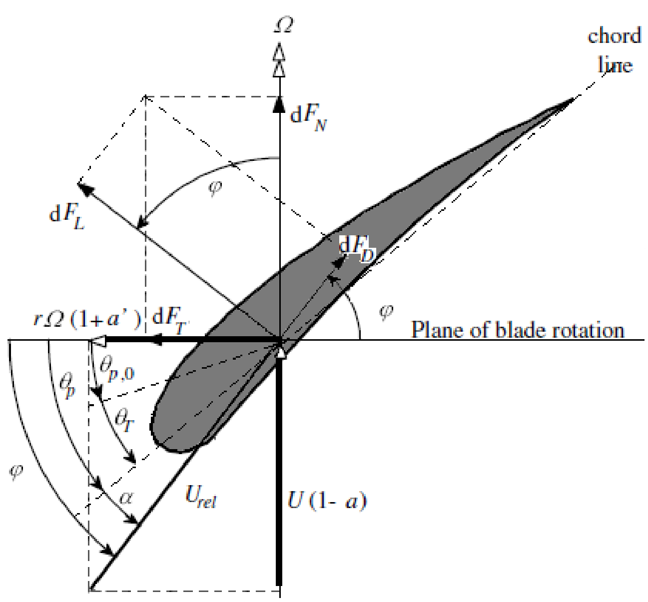

Figure 2: HAWT Blade Geometry [Manwell et al., 2002]

Tip and hub losses are added to the BEM theory. Prandtl modeled the tip loss effect with equation 14 [Glauert, 1935; Moriarty & Hansen, 2005]. A hub loss correction factor is utilized in equation 15. Therefore, for a given blade element, the local aerodynamics depends on the effects from both losses[Moriarty & Hansen, 2005]. F, the total loss correction factor (equation 16), is obtained by the multiplication of the tip loss correction factor, F_{tip}, and hub loss correction factor, F_{hub}. Tip and hub loss correction factors are found as,

$$F_{tip} = \frac{2}{\pi} cos^{-1}(e^{-\frac{B}{2}\frac{R-r}{r \sin\varphi}}) \quad (14)$$

$$F_{hub} = \frac{2}{\pi} cos^{-1}(e^{-\frac{B}{2}\frac{r-Rhub}{r \sin\varphi}}) \quad (15)$$

$$F = F_{tip}F_{hub} \quad (16)$$

The elemental total torque and thrust of turbine rotor are calculated directly by equations (1 and 2) or (3 and 4) when the axial, a , and tangential, a', induction factors are determined. The expressions for these factors are obtained by equating the thrust equations (1 and 3) and momentum equations (2 and 4). This results in the following equations for the axial and tangential induction factors, respectively.

$$a = [1 + \frac{4F\sin^2\varphi}{\sigma C_n}]^{-1} \quad (17)$$

$$a' = [-1 + \frac{4F\sin\varphi\cos\varphi}{\sigma C_t}]^{-1} \quad (18)$$

where σ is the local solidity of the rotor, which is calculated as

$$\sigma = \frac{Bc}{2\pi r} \quad (19)$$

The induction factors are estimated by an iterative process. In the iterative process, when the desired limitations and the convergence criteria for the values of induction factors are achieved. Then, the estimated axial and tangential induction factors are used to calculate elemental lift and drag forces. Afterwards, these aerodynamic forces are utilized to find the elemental normal (thrust) and tangential forces. Lastly, these forces are employed to obtain the elemental total thrust and torque of the turbine.

BEM theory becomes inaccurate when the axial induction factor exceeds the critical axial induction factor, a_c. This corresponds to a turbine operation in turbulent wake state. The flow behavior in that state cannot be estimated with the BEM approximations. Therefore, to get realistic results, an empirical relationship between the axial induction factor and the thrust coefficient is a necessity. A number of empirical corrections are available in literature, Glauert [Manwell et al., 2002], Buhl [Buhl, 2005], Spera [Hansen, 2008]. This study uses Spera's correction (equations 20 and 21) to calculate the axial induction factor. Here, the critical value for the axial induction factor is taken as 0.2. Therefore, the new axial induction factor is calculated by equations 20 and 21 when the last determined axial induction factor in the iteration process is larger than 0.2.

$$\mathrm{a} = \frac{1}{2}\left[2 + \mathrm{K}(1 - 2\mathrm{a_c}) - \sqrt{(\mathrm{K}(1 - 2\mathrm{a_c}) + 2)^2 + 4(\mathrm{Ka_c^2} - 1)}\right] \quad (20)$$

where the variable K is defined as

$$\mathrm{K} = \frac{4\mathrm{F}\sin^2\varphi}{\sigma C_n} \quad (21)$$

Integrating the equations (1 and 2) or (3 and 4) throughout the blade span gives the total aerodynamic thrust and torque of the turbine. Considering the rotor shaft speed, the power produced by the turbine is estimated by the equation 22.

$$P = \tau_{aero}\Omega \quad (22)$$

Precone and Tilt Angle Modelling

Modern wind turbines have rotors with a fixed precone angle and a nacelle with a fixed tilt angle. Besides, they have a nacelle with yawing capability into the wind. The utilized NREL 5 MW turbine has these properties, 2.5 degree-precone and 5 degree-tilt angles [Jonkman et al., 2009]. Moreover, there is a 120 degree-azimuth angle between each blade, which is not taken into account until now. In order to add all these features, some additional coordinate systems are employed in the developed model (Figure 3). When a turbine rotor is yawed with an angle towards the freestream velocity, the axial induction factor is also corrected by the skewed wake correction formula of Pitt and Peters [Pitt & Peters, 1981;Moriarty & Hansen, 2005]   as follows:

$$a_{skew} = a[1 + \frac{15\pi}{32}\frac{r}{R}\tan\frac{X}{2}\sin\Lambda] \tag{23}$$

where X and Λ represent the wake skew angle of the turbine rotor, azimuth angles of the wind turbine blades, respectively. The wake skew angle is estimated approximately using the relationship of Burton [Burton, Jenkins, Sharpe & Bossanyi, 2011, Moriarty & Hansen, 2005].

$$X = (0.6a + 1)\Psi \tag{24}$$

where Ψ is the wind turbine yaw angle seen in Figure 3-b.

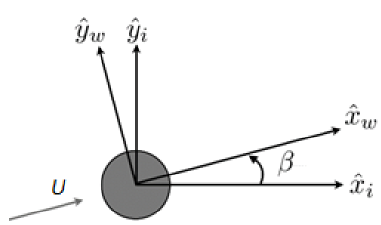

a) Inertial and Wind-aligned Coordinate Systems

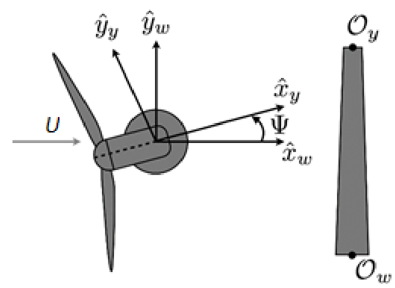

b) Wind-aligned and Yaw-aligned Coordinate Systems

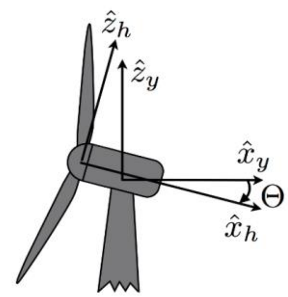

c) Yaw-aligned and Hub-aligned Coordinate Systems

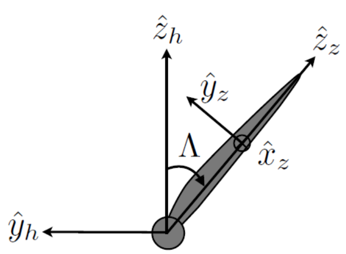

d) Hub-aligned and Azimuth-aligned Coordinate Systems

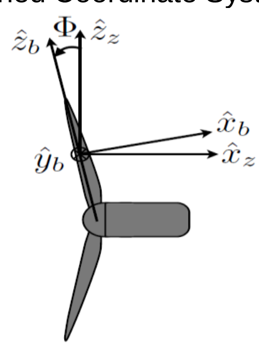

e) Azimuth-aligned and Blade-aligned Coordinate Systems

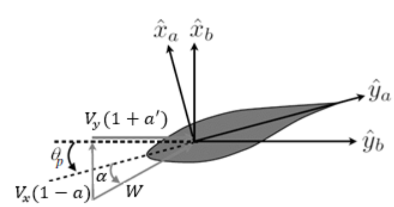

f) Blade-aligned and Airfoil-aligned Coordinate Systems

Figure 3: Wind Turbine Coordinate Systems [Ning, 2013]

Considering the conventional static rotor geometry with the precone and tilt angles exposed to a uniform freestream velocity, U which points in the $\hat{x}_i$ axis of the Inertial Coordinate System [Ning et al., 2015], the other velocity components, V_x and V_y at the Blade-aligned Coordinate Systems turn out to be as followings due to the transformation of freestream velocity from the Inertial Coordinate System.

$$V_x = U(\cos\Phi\cos\theta\cos\Psi + \sin\Phi(\cos\Lambda\sin\theta\cos\Psi + \sin\Lambda\sin\Psi)) \tag{25}$$

$$V_y = U(\sin\Lambda\sin\theta\cos\Psi - \cos\Lambda\sin\Psi) + \Omega r\cos\Phi \tag{26}$$

Therefore, U_{rel} equation (11) has changed into W in equation 27, and inflow angle, φ equation (12) has turned into equation 28. Then, the velocity W in Figure 3-f is calculated by the equation 27. Further, the transformation (equations 7 and 8), is carried out inside the iteration process.

$$W = \sqrt{(V_x(1-a))^2 + (V_y(1+a'))^2} \tag{27}$$

$$\varphi = \tan^{-1}\frac{V_x(1-a)}{V_y(1+a')} \tag{28}$$

The elemental aerodynamic forces at Blade-aligned Coordinate System are found by using equations 9 and 10 and then considering the equations 7 and 8, elemental torque and thrust are obtained from equations 5 and 6. In all of these equations, W is used, instead of U_{rel}. These elemental torque and thrust are later integrated for every blade span to calculate the total thrust and torque of the turbine with consideration of rotor precone angle, and azimuthal orientation of each blade.

Iteration Process and Corrections

This subsection explains the step by step iteration process and the application of corrections to calculate elemental torque and thrust of a turbine blade. This is summarized as follows:

1. Start the iteration loop by Initializing a and a' with zero.
2. Calculate the inflow angle, φ by equation 28.
3. Calculate the angle of attack, α by equation 13.
4. Calculate the hub loss factor, F_{hub} by equation 15.
5. Calculate the tip loss factor, F_{tip} by equation 14.
6. Calculate the total loss factor, F by equation 16.
7. Get the aerodynamic data, C_l, C_d corresponding to the calculated angle of attack,α
8. Calculate the normal and tangential force coefficients, C_n, C_t by equation 7, 8.
9. Calculate the local solidity, σ by equation 19.
10. Calculate the axial induction factor, a by equation 17
11. Apply Spera's correction by equation 20 and 21, if $a \geq a_c$.
12. Calculate the tangential induction factor, a' by equation 18.
13. if a and a' has changed more than convergence criteria, go to step 2 and continue to iterate until the criteria is satisfied.
14. Apply the skewed wake correction by equations 23, 24 if $\Psi > 0$.
15. Calculate elemental lift, dF_L and drag, dF_D forces by equations 9 and 10.
16. Calculate elemental normal (thrust), dF_N and tangential, dF_T forces by equations 5 and 6.

Dynamic Wind Turbine Modeling

The turbine has been modeled as a single mass as illustrated in Figure 4. The rotor torque acts in the opposite direction to that of the generator.

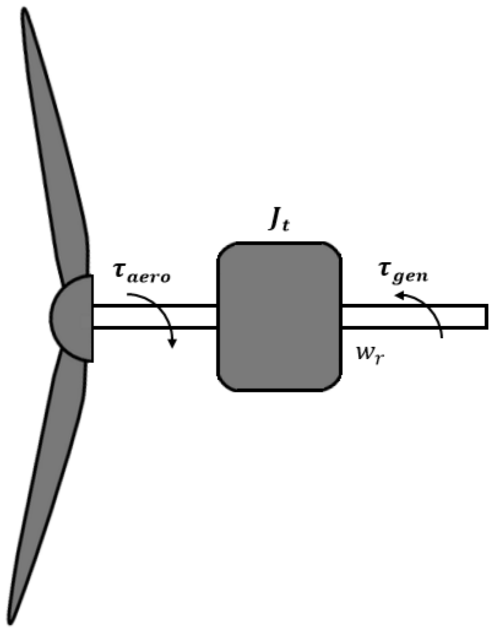

Figure 4: Wind Turbine Model Dynamics with One Mass

Hence, when a single mass turbine model with a perfectly stiff, frictionless shaft is taken into consideration, the dynamics of the variable speed turbine from Newton 2^{nd} law of motion becomes as equation 29.

$$J_t\dot{\Omega} = \tau_{aero} - \tau_{gen} \tag{29}$$

where J_t is the total inertia of the turbine system and found as

$$J_t = J_{rotor} + N_{gear}^2 J_{gen} \tag{30}$$

MODEL VALIDATION and CONCLUSIONS

For the validation purpose, the model power outputs at different freestream velocities and various blade pitch angles (Figure 5) are compared with those of [Galvani et al., 2016]. To compare the results, rotor precone, nacelle tilt and yaw angles are all set to zero since the reference model[Galvani et al., 2016] is simple and does not includes all these features. As seen from the results (Figure 5), power predictions of the current aerodynamic model and those of [Galvani et al., 2016] at different blade pitch angles give almost the same power outputs at low freestream velocities, while there is minor difference in power outputs at high freestream velocities.

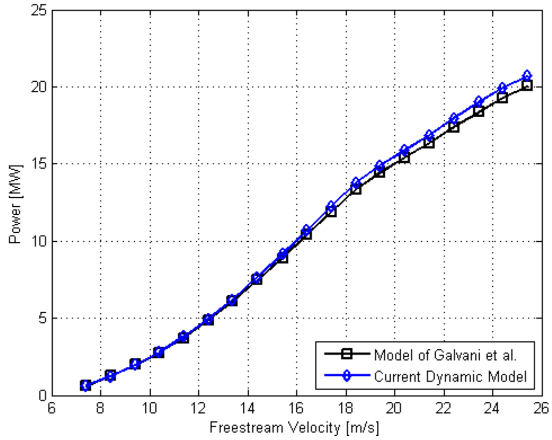

a) Power Output at 6 Degree-Blade Pitch Angle

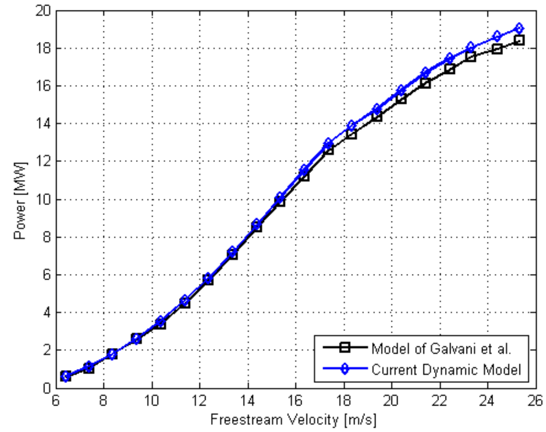

b) Power Output at 4 Degree-Blade Pitch Angle

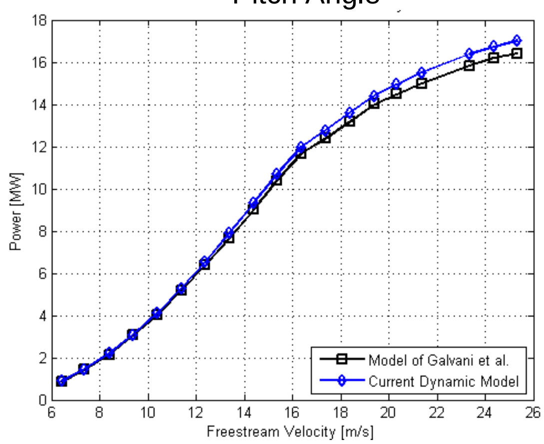

c) Power Output at 2 Degree-Blade Pitch Angle

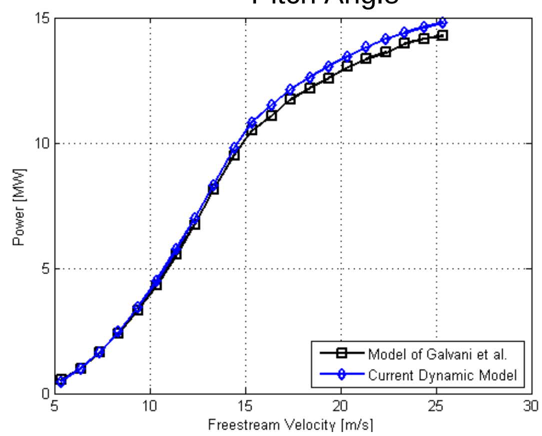

d) Power Output at 0 Degree-Blade Pitch Angle

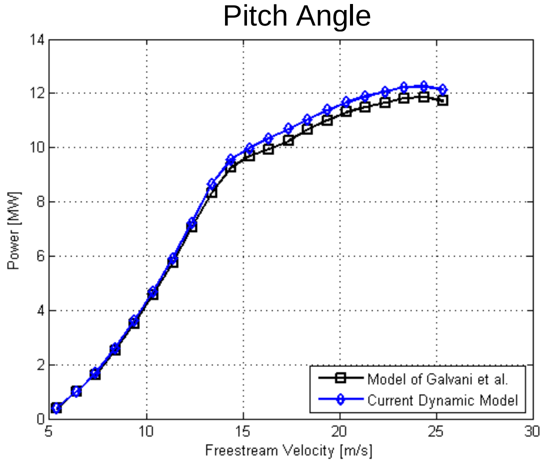

e) Power Output at -2 Degree-Blade Pitch Angle

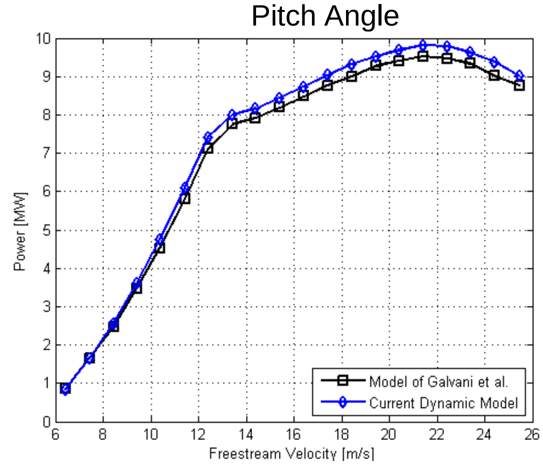

f) Power Output at -4 Degree-Blade Pitch Angle

Figure 5: Power Outputs of 5 MW Turbine at Various Pitch Angles

The probable reasons for the difference may be explained as follows:

Before everything else, the density used in the reference study is not given explicitly. But, considering the usage of same density, 1.255 $\mathrm{kg/m^3}$[Jonkman et al., 2009], the difference is not caused by one parameter. It is a combination of followings. Firstly, the selected convergence tolerance and blade element number are different in each model. The developed model here uses a convergence tolerance value of 0.005, a blade element number of 17, while those of Galvani et al. are 0.01 and 100, respectively. Secondly, the hub loss effect is not included in reference model, but it is available in the developed model since the turbine model is incomplete without this effect. The difference may also depend on how the turbine blade is divided into elements, how the integration for the thrust and torque are carried out through the blade span and whether the airfoils distributions are taken into account carefully. Due to all of above, a minor difference in power output of both models appears at high freestream velocities, while almost no difference at low freestream velocities.

After the model validation, the developed model has been turned into a dynamic model by applying the Newton 2 law of motion. Except for this application, which is realized in Simulink program, all of above are carried out by MATLAB software.

Consequently, the aerodynamic model in the developed simulation model shows similarities to PROP code [Wilson & Lissaman, 1974], AeroDyn [Moriarty & Hansen, 2005] and WT_Perf [Platt & Buhl, 2012] to a certain extend. As final adjustments for the developed simulation model, freestream velocity, each blade pitch angle, and rotor angular velocity are selected as inputs, while thrust, torque, power, and their respective coefficients, along with TSR are chosen as turbine outputs. Yaw, precone and tilt angles and more may also be defined as inputs and more outputs may be obtained from the model when desired.

References

Buhl, M. L. (2005). *A New Empirical Relationship between Thrust Coefficient and Induction Factor for the Turbulent Windmill State A New Empirical Relationship between Thrust Coefficient and Induction Factor for the Turbulent Windmill State*. *Technical Report NREL/TP-500-36834*.

Burton, T., Sharpe, D., Jenkins, N., & Bossanyi, E. (2001). *Wind Energy Handbook*. West Sussex, England: John Wiley & Sons, Ltd.

Burton, T., Jenkins, N., Sharpe, D., and Bossanyi, E.(2011), Wind Energy Handbook, Wiley, (2nd Edi).

Ceyhan, Ö. (2008). *Aerodynamic Design and Optimization of Horizontal Axis Wind Turbines by Using BEM Theory and Genetic Algorithm*. Middle East Technical University.

Erich, H. (2006). *Wind Turbines-Fundamentals, Tecnologies, Application, Economics*. *Spectrum* (2nd Edi). Germany.

Galvani, P. A., Sun, F., & Turkoglu, K. (2016). Aerodynamic Modelling of the NREL 5-MW Wind Turbine for Nonlinear Control System Design: A case Study Based on Real-Time Nonlinear Receding Horizon Control. *Aerospace 2016*. https://doi.org/10.3390/aerospace3030027

Glauert, H. (1935). *“Airplane Propellers.”* Aerodynamic Theory (W. F. Durand, ed.), Div. L, Chapter XI. Berlin:Springer Verlag.

GWEC. (2016). *Global Status of Wind Power in 2016*. Retrieved from http://www.gwec.net/wp-content/uploads/2017/05/Global-Status-2016.pdf

Hansen, M. O. L. (2008). *Aerodynamics of Wind Turbines* (2th Edit.). Earthscan.

Jonkman, J., Butterfield, S., Musial, W., & Scott, G. (2009). *Definition of a 5-MW Reference Wind Turbine for Offshore System Development*. *Technical Report NREL/TP-500-38060*.

Manwell, J. F., McGowan, J. G., & Rogers, A. L. (2002). *Wind Energy Explained-Theory, Design and Application*. John Wiley & Sons Ltd.

Moriarty, P. J., & Hansen, A. C. (2005). *AeroDyn Theory Manual, NREL/TP-500-36881, Golden, Colorado: National Renewable Energy Laboratory*.

Pitt, D.M.; Peters, D.A. 1981. “Theoretical Prediction of Dynamic-Inflow Derivatives.” Vertica, 5(1), March.

Ning, S. A. (2013). *CCBlade Documentation, Release 0.1.0*.

Ning, S. A., Hayman, G., Damiani, R., & Jonkman, J. (2015). Development and Validation of a New Blade Element Momentum Skewed-Wake Model within AeroDyn. In *AIAA Science and Technology Forum and Exposition 2015*. Retrieved from http://www.nrel.gov/docs/fy15osti/63217.pdf

Pao, L. Y., & Johnson, K. E. (2009). A Tutorial on the Dynamics and Control of Wind Turbines and Wind Farms. In *2009 American Control Conference* (pp. 2076–2089). Hyatt Regency Riverfront, St. Louis, MO, USA. https://doi.org/10.1109/ACC.2009.5160195

Platt, A. D., & Buhl, M. L. (2012). *WT_Perf User Guide for Version 3.05.00*.

Singh, M., & Santoso, S. (2011). *Dynamic Models for Wind Turbines and Wind Power Plants Dynam,NREL/SR-5500-52780, Golden, Colorado: National Renewable Energy Laboratory*.

Wilson, R. E., & Lissaman, P. B. S. (1974). *Applied Aerodynamics of Wind Power Machines*.